

Large-Amplitude Oscillations of Oblique Panels with an Initial Curvature

J L NOWINSKI*

University of Delaware, Newark, Del

Von Kármán field equations for flexible oblique plates with an initial curvature are extended to a dynamical case. Using series representation of initial and additional deflections and Galerkin's procedure, the governing equation for an admissible mode time function is established. Using this single assumed modal deflection, and assuming built-in edge free to move in the inplane directions, the following particular cases are discussed: buckling of an oblique plate under uniaxial compressive load, free linear vibrations of a square plate, large deflections of a uniformly loaded square plate, snap-through phenomena of a curved oblique plate under uniform transverse load, and free nonlinear vibrations. A numerical example concerning a rhombic plate is discussed in more detail. The well-known fact of a decrease of the period of nonlinear vibrations with an increasing amplitude is corroborated, this relation being less pronounced for larger sweep angles.

Introduction

OBlique panels find frequent application in technology of modern flying vehicles, mainly as standard structural elements of swept-back wings of airplanes. They appear in the form of flexible plates shaped as skew parallelograms, initially slightly curved and supported at the periphery by stringers and ribs usually parallel to the direction of flight. Because of their flexibility, buckling phenomena involving flat oblique panels have been investigated to certain extent in the last decade, mostly with regard to a uniform uniaxial inplane compression and shear (compare, e.g., Refs 1-6). On the other hand, dynamical phenomena have attracted less attention, and in particular those which lead to oscillations with a large amplitude. In fact, the author could not trace any paper pertinent to the latter case.[†] Analysis of such problems, however, may be of importance, for instance, in connection with oscillations of swept-back wings at supersonic flight.

As far as nonlinear oscillations of rectangular panels are concerned, Grigoliuk⁷ in 1955 analyzed this problem for a specific type of support applying Galerkin's method to von Kármán's equations extended to the dynamical case. In 1956, Chu and Heumann⁸ studied vibrations of freely supported plates by means of a perturbation procedure and the principle of conservation of energy. Making use of an approximate analysis offered by the Berger method, Nash and Modeer,⁹ in 1959, investigated the nonlinear behavior of vibrating rectangular plates, and in 1962 Hassert and Nowinski¹⁰ discussed this problem with regard to an orthogonally anisotropic material and a simple support.

In the present paper, an investigation is made of the transverse large-amplitude vibrations of oblique plates with double initial curvature. Von Kármán field equations are extended to embrace the dynamical case, and Galerkin's procedure is used furnishing the governing equation for a lowest-mode time function. Assuming a particular type of support, buckling of oblique plates under uniaxial compressive load and large transverse deflections under a uniform load are discussed. Free linear and free nonlinear vibrations are investigated in more detail. A numerical example involving a rhombic plate is given.

Received December 9, 1963; revision received March 26, 1964. The results were obtained in the course of research supported by a grant of the National Science Foundation.

* Professor of Mechanical Engineering, Department of Mechanical Engineering.

[†] It is likely that the search was not extensive enough.

1 Formulation of the Problem

Let us consider an oblique initially doubly curved elastic plate of length a and width b , the angle of the sweptback being φ and the constant thickness of the plate being h (Fig 1). At the center of the plate let us locate the origin of two Cartesian coordinate frames: one rectangular x, y , and one oblique ξ, η related to each other by means of the mapping

$$\xi = x/\cos\varphi \quad \eta = -tg\varphi x + y \quad (1.1)$$

Since, in the oblique coordinate system ξ, η , the Laplace operator has the form

$$\nabla_{\xi\eta}^2 = \frac{1}{\cos^2\varphi} \left[\frac{\partial^2}{\partial \xi^2} - 2\sin\varphi \frac{\partial^2}{\partial \xi \partial \eta} + \frac{\partial^2}{\partial \eta^2} \right] \quad (1.2)$$

the well-known von Kármán field equations (Ref 17, pp 348-351) extended to the dynamical case and to small initial curvature appear as

$$F(w, \phi) \equiv (D/h)\nabla^2\nabla^2 w - L(w, \phi) - L(w_0, \phi) - (q/h) + \rho(\partial^2 w / \partial t^2) = 0 \quad (1.3)$$

$$(1/E)\nabla^2\nabla^2 \phi = -\frac{1}{2}L(w, w) - L(w_0, w) \quad (1.4)$$

where, for conciseness, the subscripts at the nabla operators have been omitted. In the foregoing equations, D , as usual, stands for the bending rigidity of the plate, ρ for its mass density, $q = q(\xi, \eta)$ is the intensity of the external load, $w_0 = w_0(\xi, \eta)$ the initial deflection of the plate, $w = w(\xi, \eta, t)$ an additional deflection produced by the load, and

$$L(w, \phi) = \frac{1}{\cos^2\varphi} \left(\frac{\partial^2 w}{\partial \xi^2} \frac{\partial^2 \phi}{\partial \eta^2} + \frac{\partial^2 w}{\partial \eta^2} \frac{\partial^2 \phi}{\partial \xi^2} - 2 \frac{\partial^2 w}{\partial \xi \partial \eta} \frac{\partial^2 \phi}{\partial \xi \partial \eta} \right) \quad (1.5)$$

We note that the skew membrane stresses σ_ξ , σ_η , and $\tau_{\xi\eta}$ may be expressed by means of the stress function $\phi(\xi, \eta)$ as

$$\begin{aligned} \sigma_\xi &= (1/\cos\varphi)(\partial^2 \phi / \partial \eta^2) \\ \sigma_\eta &= (1/\cos\varphi)(\partial^2 \phi / \partial \xi^2) \\ \tau_{\xi\eta} &= -(1/\cos\varphi)(\partial^2 \phi / \partial \xi \partial \eta) \end{aligned} \quad (1.6)$$

In this form, the stresses (1.6) satisfy the equations of balance of forces in the directions tangent to the middle surfaces of the panel, provided the inertia terms inherent with the motion in the middle surface are disregarded. Such an assumption has been corroborated (see, e.g., Ref 8) and is commonly accepted in problems in which vibrations take

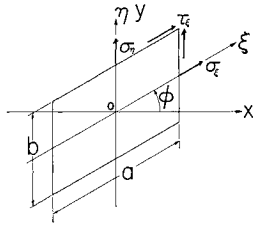


Fig 1 Geometry of the plate

place, principally in the direction perpendicular to the middle surface

To the governing field equations [(1.3) and (1.4)] we must adjoin the initial and boundary conditions to be discussed later. This completes the formulation of the problem that is now reduced to the integration of a system of two nonlinear differential equations in combination with some prescribed conditions. Apparently, the difficult problem under investigation may be solved only by using an approximate technique. For this purpose, assume first, for definiteness, that the plate is built-in at the periphery, that is,

$$\begin{aligned} w[\pm(a/2), \eta, t] &= 0 & w[\xi, \pm(b/2), t] &= 0 \\ (\partial w / \partial \xi)[\pm(a/2), \eta, t] &= 0 & (\partial w / \partial \eta)[\xi, \pm(b/2), t] &= 0 \end{aligned} \quad (1.7)$$

at each time $t \geq 0$. We now represent the deflection of the plate in the following separable form:

$$w(\xi, \eta, t) = \sum_{\nu, \mu} A_{\nu\mu} \tau_{\nu\mu}(t) \varphi_{\nu\mu}(\xi, \eta) \quad (1.8)$$

where $\tau_{\nu\mu}(t)$ are unknown functions of time only to be determined in the sequel, and $\varphi_{\nu\mu}(\xi, \eta)$ are suitably chosen spacial functions which satisfy the boundary conditions (1.7).[†] In what follows, we pose, without relevant loss in generality,

$$\varphi_{\nu\mu}(\xi, \eta) = [1 + (-1)^{\nu+1} \cos \alpha_\nu \xi][1 + (-1)^{\mu+1} \cos \beta_\mu \eta] \quad (1.9)$$

where $\alpha_\nu = 2\pi\nu/a$ and $\beta_\mu = 2\pi\mu/b$.

The initial deflection of the plate is expanded into the Fourier series

$$w_0(\xi, \eta) = \sum_{\nu, \mu} B_{\nu\mu} \varphi_{\nu\mu}^0(\xi, \eta) \quad (1.10)$$

in which $B_{\nu\mu}$ clearly denote known constant coefficients, and the functions $\varphi_{\nu\mu}^0(\xi, \eta)$ are selected in the form analogous to (1.9). To avoid complications in writing, in what follows we confine ourselves to a single term in each series (1.8) and (1.10), thus obtaining

$$w(\xi, \eta, t) = A\tau(t)(1 + \cos \alpha \xi)(1 + \cos \beta \eta) \quad (1.11)$$

$$w_0(\xi, \eta) = A_0(1 + \cos \alpha \xi)(1 + \cos \beta \eta) \quad (1.12)$$

where now $\alpha = 2\pi/a$ and $\beta = 2\pi/b$. Of course, at a considerable expense of computational work, it is possible to employ more terms of the series (1.8) and (1.10) than one and to increase the generality as well as, to some extent, the accuracy of the results. Nonetheless, even drastically truncated equations (1.11) and (1.12) may furnish some useful results of a specific nature although subject to limitations pertinent to a single mode approximation.

2 Determination of Membrane Stresses

We now proceed to determine the stress function $\phi(\xi, \eta, t)$ and the membrane stresses in terms of ϕ . For this purpose, we substitute Eqs. (1.11) and (1.12) into the right-hand

member of the governing equation (1.4) and find, with a little manipulation, the following particular integral of (1.4) suitable for the problem under investigation:

$$\begin{aligned} \phi(\xi, \eta, t) = & -\tau^* \cos^2 \varphi \left[\frac{\cos \alpha \xi}{\alpha^4} + \frac{\cos \beta \eta}{\beta^4} + \right. \\ & \frac{\cos 2\alpha \xi}{16\alpha^4} + \frac{\cos 2\beta \eta}{16\beta^4} + \lambda_1(\cos \alpha \xi \cos \beta \eta - \\ & \kappa_1 \sin \alpha \xi \sin \beta \eta) + \lambda_2(\cos 2\alpha \xi \cos \beta \eta - \\ & \kappa_2 \sin 2\alpha \xi \sin \beta \eta) + \lambda_3(\cos \alpha \xi \cos 2\beta \eta - \\ & \left. \kappa_3 \sin \alpha \xi \sin 2\beta \eta) \right] + \cos \varphi \left(p_\xi \frac{\eta^2}{2} + p_\eta \frac{\xi^2}{2} - p_{\xi\eta} \xi \eta \right) \quad (2.1) \end{aligned}$$

In the preceding equation, p_ξ , p_η , and $p_{\xi\eta}$ denote oblique normal and shear stresses, constant throughout the region of the plate, eventually functions of time. Moreover,

$$\tau^* = EA\alpha^2\beta^2[(A/2)\tau^2 + A_0\tau] \quad (2.2)$$

$$\begin{aligned} \lambda_1 &= \frac{2}{(\alpha^2 + \beta^2)^2 + 4\alpha^2\beta^2 \sin^2 \varphi - 4\alpha\beta(\alpha^2 + \beta^2)\kappa_1 \sin \varphi} \\ \lambda_2 &= \frac{1}{(4\alpha^2 + \beta^2)^2 + 16\alpha^2\beta^2 \sin^2 \varphi - 8\alpha\beta(4\alpha^2 + \beta^2)\kappa_2 \sin \varphi} \\ \lambda_3 &= \frac{1}{(\alpha^2 + 4\beta^2)^2 + 16\alpha\beta^2 \sin^2 \varphi - 8\alpha\beta(\alpha^2 + 4\beta^2)\kappa_3 \sin \varphi} \end{aligned} \quad (2.3.1)$$

$$\left. \begin{aligned} \kappa_1 &= \frac{4\alpha\beta(\alpha^2 + \beta^2) \sin \varphi}{(\alpha^2 + \beta^2)^2 + 4\alpha\beta^2 \sin^2 \varphi} \\ \kappa_2 &= \frac{8\alpha\beta(4\alpha^2 + \beta^2) \sin \varphi}{(4\alpha^2 + \beta^2)^2 + 16\alpha^2\beta^2 \sin^2 \varphi} \\ \kappa_3 &= \frac{8\alpha\beta(\alpha^2 + 4\beta^2) \sin \varphi}{(\alpha^2 + 4\beta^2)^2 + 16\alpha^2\beta^2 \sin^2 \varphi} \end{aligned} \right\} \quad (2.3.2)$$

With these in mind, a substitution of (2.1) into (1.6) yields the components of the membrane stresses in the following final form:

$$\left. \begin{aligned} \sigma_\xi &= \tau^* \cos \varphi \left[\frac{\cos \beta \eta}{\beta^2} + \frac{\cos 2\beta \eta}{4\beta^2} + \right. \\ & \lambda_1 \beta^2 \cos \alpha \xi \cos \beta \eta - \kappa_1 \lambda_1 \beta^2 \sin \alpha \xi \sin \beta \eta + \\ & \lambda_2 \beta^2 \cos 2\alpha \xi \cos 2\beta \eta - \kappa_2 \lambda_2 \beta^2 \sin 2\alpha \xi \sin 2\beta \eta + \\ & \left. 4\lambda_3 \beta^2 \cos \alpha \xi \cos 2\beta \eta - 4\lambda_3 \kappa_3 \beta^2 \sin \alpha \xi \sin 2\beta \eta \right] + p_\xi \\ \sigma_\eta &= \tau^* \cos \varphi \left[\frac{\cos \alpha \xi}{\alpha^2} + \frac{\cos 2\alpha \xi}{4\alpha^2} + \right. \\ & \lambda_1 \alpha^2 \cos \alpha \xi \cos \beta \eta - \kappa_1 \lambda_1 \alpha^2 \sin \alpha \xi \sin \beta \eta + \\ & 4\lambda_2 \alpha^2 \cos 2\alpha \xi \cos \beta \eta - 4\lambda_2 \kappa_2 \alpha^2 \sin 2\alpha \xi \sin \beta \eta + \\ & \left. \lambda_3 \alpha^2 \cos \alpha \xi \cos 2\beta \eta - \lambda_3 \kappa_3 \alpha^2 \sin \alpha \xi \sin 2\beta \eta \right] + p_\eta \\ \tau_{\xi\eta} &= \tau^* \alpha \beta \cos \varphi [\lambda_1 \sin \alpha \xi \sin \beta \eta - \\ & \lambda_1 \kappa_1 \cos \alpha \xi \cos \beta \eta + 2\lambda_2 \sin 2\alpha \xi \sin \beta \eta - \\ & 2\lambda_2 \kappa_2 \cos 2\alpha \xi \sin \beta \eta + 2\lambda_3 \sin \alpha \xi \sin 2\beta \eta - \\ & \left. 2\lambda_3 \kappa_3 \cos \alpha \xi \cos 2\beta \eta] + p_{\xi\eta} \end{aligned} \right\} \quad (2.4)$$

It may be easily shown upon integration of Eqs. (2.4) along the edges of the plate that the contribution of the first member at the right-hand side of Eqs. (2.4), enclosed in brackets

[†] For future calculations, it is expedient to separate in (1.8) the constant coefficients $A_{\nu\mu}$ from the associated time functions

to the average stresses at the corresponding edge of the plate is nil. Hence the constant stresses p_ξ , p_η , and $p_{\xi\eta}$ may be regarded as the average edge membrane stresses.

To be more definite, assume that the clamping of the edges of the plate does not prevent free inplane motions. This yields the following complementary boundary conditions:

$$p_\xi = p_\eta = p_{\xi\eta} = 0 \quad (2.5)$$

assumed in pertinent portions of the following development

3 Governing Time Equation

We now turn our attention to the only remaining field equation of motion (1.3) to which we apply the procedure of Galerkin (compare, e.g., Ref. 7 and Ref. 11, p. 58). We proceed in the following way. Upon substituting from (1.11, 1.12, and 2.1) into (1.3), we multiply $F(w, \phi)$ by the spacial part of the coordinate function (1.11), that is, by $(1 + \cos \alpha \xi)(1 + \cos \beta \eta)$, and integrate the result over the region $-(a/2) \leq \xi \leq (a/2)$, $-(b/2) \leq \eta \leq (b/2)$. A longer but elementary calculation yields the following nonlinear differential equation of the second order for the time function τ :

$$\begin{aligned} 9\rho A \frac{d^2\tau}{dt^2} + \left\{ \frac{AD}{h \cos^4 \varphi} [3\alpha^4 + 3\beta^4 + 2\alpha^2\beta^2(1 + 2\sin^2 \varphi)] + \right. \\ \left. \frac{3A}{\cos \varphi} (\alpha^2 p_\xi + \beta^2 p_\eta) + EA_0^2 \alpha^2 \beta^2 \Omega \right\} \tau + \\ \frac{3}{2} EA^2 A_0 \alpha^2 \beta^2 \Omega \tau^2 + \frac{1}{2} EA^3 \alpha^2 \beta^2 \Omega \tau^3 - \frac{4q}{h} + \\ \frac{3}{\cos \varphi} (\alpha^2 p_\xi + \beta^2 p_\eta) A_0 = 0 \quad (3.1.1) \end{aligned}$$

in which

$$\begin{aligned} \Omega = \alpha^2 \left[\frac{17}{8\beta^2} + (2\lambda_1 + \lambda_2 + 2\lambda_3)\beta^2 \right] + \\ \beta^2 \left[\frac{17}{8\alpha^2} + (2\lambda_1 + 2\lambda_2 + \lambda_3)\alpha^2 \right] + \\ 2(\lambda_1 + \lambda_2 + \lambda_3)\alpha^2 \beta^2 \quad (3.1.2) \end{aligned}$$

providing the loading function $q(\xi, \eta, t)$ is independent of the space coordinates, thus representing a uniform loading eventually varying with time.

At this stage, it is expedient to introduce dimensionless variables by means of the following definitions:

$$\left. \begin{aligned} \sigma &= h\alpha^2 \left(\frac{E}{\rho} \right)^{1/2} t & A^*(t) &= U(\sigma) & A^* &= 4 \frac{A}{h} \\ A_0^* &= 4 \frac{A_0}{h} & \mu &= \frac{\beta}{\alpha} = \frac{a}{b} & p_\xi^* &= \frac{p_\xi}{Eh^2 \alpha^2} \\ p_\eta^* &= \frac{p_\eta}{Eh^2 \alpha^2} & q^* &= \frac{qa^4}{Eh^4} \end{aligned} \right\} \quad (3.2)$$

An inspection of (3.2) reveals that A_0^* and A^* denote non-dimensional initial and additional deflection at the center of the plate, respectively ($A_0^* = [w_0(0)/h]$, $A^* = [w(0)/h]$). Upon substitution from (3.2), the governing time equation (3.1) takes the following final form:

$$\begin{aligned} \frac{d^2 U}{d\sigma^2} + u_1 U + u_2 U^2 + u_3 U^3 + \\ \frac{1}{3 \cos \varphi} (p_\xi^* + \mu^2 p_\eta^*) A_0^* - \frac{q^*}{9\pi^4} = 0 \quad (3.3) \end{aligned}$$

where

$$\left. \begin{aligned} u_1 &= \frac{1}{36} \left\{ \frac{1}{3(1 - \nu^2) \cos^4 \varphi} \times \right. \\ &\quad [3 + 3\mu^4 + 2\mu^2(1 + 2\sin^2 \varphi)] + \\ &\quad \left. \frac{1}{4} \mu^2 \Omega (A_0^*)^2 + \frac{12}{\cos \varphi} (p_\xi^* + \mu^2 p_\eta^*) \right\} \\ u_2 &= \frac{1}{96} \mu^2 \Omega A_0^* & u_3 &= \frac{1}{288} \mu^2 \Omega \\ \Omega &= \mu^2 \left(\frac{17}{8\mu^4} + 2\lambda_1^* + \lambda_2^* + \lambda_3^* + \frac{17}{8} \right) \\ \lambda_1^* &= \frac{2}{(1 + \mu^2)^2 + 4\mu^2 \sin^2 \varphi - 4\mu\kappa_1(1 + \mu^2) \sin \varphi} \\ \lambda_2^* &= \frac{1}{(4 + \mu^2)^2 + 16\mu^2 \sin^2 \varphi - 8\mu\kappa_2(4 + \mu^2) \sin \varphi} \\ \lambda_3^* &= \frac{1}{(1 + 4\mu^2)^2 + 16\mu^2 \sin^2 \varphi - 8\mu\kappa_3(1 + 4\mu^2) \sin \varphi} \end{aligned} \right\} \quad (3.4)$$

Equation (3.3) provides a background for the entire discussion that follows. For a more detailed development of the ideas, let us now specialize Eq. (3.3) to refer to the following particular cases.

A Buckling of a Flat Rectangular Plate with Built-in Edges under Inplane Compressive Load

In this case we set $A_0 = \varphi = q = 0$, $\tau = 1$, and, say, $p_\eta = 0$. Since a disclosure of the critical value of the compressive force $N_\xi = \sigma_\xi h$ represents a linear problem, we disregard the powers of the amplitude A^* higher than the first. This yields, after returning to the dimensional form,

$$N_{\xi \text{ crit}} = -\frac{4\pi^2}{3} Da^2 \left(\frac{3}{a^4} + \frac{3}{b^4} + \frac{2}{a^2 b^2} \right) \quad (3.5)$$

in accord with the well-established result (compare, for instance, Timoshenko's, Ref. 12, p. 321).

For an oblique plate, the critical load becomes

$$N_{\xi \text{ crit}} = -\frac{4\pi^2}{3a^2 \cos^3 \varphi} [3(1 + \mu^4) + 2\mu^2(1 + 2\sin^2 \varphi)] \quad (3.6)$$

Apparently, the first approximation of the buckled middle surface of the plate furnished by Eq. (1.11), as a by-product of the solution of the main problem, cannot be considered an adequate representation of the true, rather complex, shape of the middle surface in the oblique case. Hence, the discrepancies between the result (3.6) and the results of more refined solutions such as derived, for instance, by Wittrick,² may be substantial. A similar situation, however, has to be noted with regard to first approximations furnished by more rigorous techniques specifically designed for solution of the buckling problem.⁸

⁸ For the values of the angle φ , equal to 15° and 30°, the error involved in (3.6) amounts to 15.5 and 57%, respectively, as compared with Ref. 2 (data taken from the graph in Fig. 2, reproduced in Ref. 5). In Ref. 6, for $\varphi = 35^\circ$, the error of the first approximation exceeds 27% (this paper treats a free support of the plate). The sensitivity of the critical compressive stress (3.6) on the angle of sweep-back, in particular for larger values of φ , becomes apparent if one notices that as $\varphi \rightarrow \pi/2$, $N_{\xi \text{ crit}} \rightarrow \infty$, thus furnishing a steep rising curve.

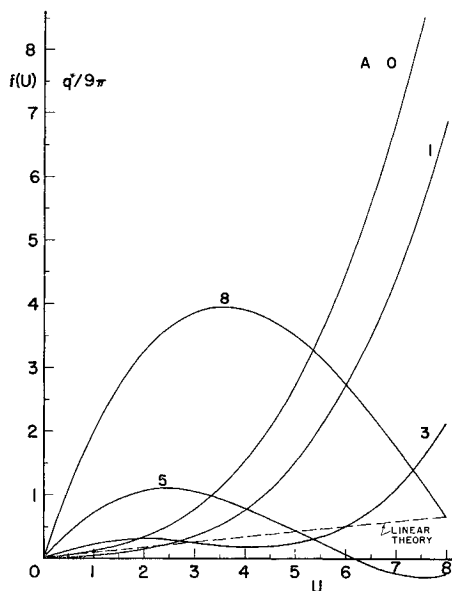


Fig. 2 Load or control function vs deflection U for a square panel and various values of initial deflection A_0^*

B Free Linear Vibrations of a Flat Square Plate with Built-in Edges

In this case, we set, as in the previous case, $A_0 = q = 0$ and $\varphi = 0$. Furthermore, we disregard τ^2 and τ^3 and drop, of course, p_ξ and p_η . Since $\alpha = \beta = 2\pi/a$, say, Eq. (3.1) becomes simply

$$(d^2\tau/dt^2) + (128/9)(\pi^4 D/\rho h a^4)\tau = 0 \quad (3.7)$$

From (3.7), the circular frequency of linear vibrations follows immediately as

$$\omega = (37.2/a^2)(D/h\rho)^{1/2} \quad (3.8)$$

in accordance with the well-known result based upon the same assumed deflection form in Ref. 13, p. 375.

C Large Deflections of a Uniformly Loaded Flat Rectangular Plate with Built-in Edges

In this particular case, we have to pose $A_0 = \varphi = 0$ and $\tau = 1$. Equation (3.3) presently becomes

$$\frac{U}{36} \left\{ \frac{1}{3(1-\eta^2)} [3(1+\mu^2) + 2\mu^2] + 12(p\xi^* + \mu^2 p\eta^*) \right\} + \frac{1}{288} \mu^2 \Omega U^3 - \frac{q^*}{9\pi^4} = 0 \quad (3.9)$$

in accordance with the result obtained, for instance, by Volmi [Ref. 11, p. 112, Eq. (2.146)].[†]

4 Snap-Through Phenomenon under a Uniform Transverse Load

We now turn our attention to the general equation (3.3) in which the time derivative is disregarded and the symbol τ substituted for by 1. Suppose that an oblique plate with a small initial curvature is acted upon by a uniformly distributed load in the direction opposite to that of the initial deflection and that the edges of the plate are free, i.e., $p_\xi^* = p_\eta^* = 0$. From (3.3) it is seen that

$$(q^*/9\pi^4) = u_1 U - u_2 U^2 + u_3 U^3 \quad (4.1)$$

where A_0^* is considered to be positive. Apparently, the

sign preceding the term $u_2 U^2$ in Eq. (4.1) has been reversed in order to account for the fact that the direction of the load is opposite to that of the initial deflection, as assumed previously. Relation (4.1) between the nondimensional intensity of load and the center deflection of the plate can be displayed graphically in a convectional way (compare, e.g., Ref. 11, p. 94 and p. 208) for various values of the amplitude of the initial deflection A_0^* as well as of the angle of sweep-back φ . Figure 2 illustrates this interdependence for a square panel. It is known that, in a certain range of the load and beyond a certain value of the initial deflection, to each value of q^* correspond, in general, three different states of equilibrium of the plate.

Denote the right-hand member of (4.1) by $f(U)$. Thus

$$f(U) = u_1 U - u_2 U^2 + u_3 U^3 \quad (4.2)$$

and the extremal values of the load q^* occur for values of $U = U_i^{xt}$, ($i = 1, 2$), which satisfy the condition $f'(U) = 0$. After making use of relations (3.4) we get

$$U_{1,2}^{xt} = A_0^* \left[1 \mp \left\{ \frac{1}{3} \left[1 - \frac{8g(\varphi)}{\mu^2 \Omega (A_0^*)^2} \right] \right\}^{1/2} \right] \quad (4.3)$$

where

$$g(\varphi) = \frac{1}{3(1-\nu^2)\cos^2\varphi} [3 + 3\mu^4 + 2\mu^2(1 + 2\sin^2\varphi)] \quad (4.3.1)$$

The equation $f'(U) = 0$ represents a quadratic parabola Q with a vertical axis, the convex side being turned toward the direction of negative ordinates, and the vertex located at

$$U_{infl} = A_0^* \quad (4.4)$$

where $f''(U) = 0$. It follows that each curve $q^*/9\pi^4 - f(U) = 0$ has an inflection point at U equal to U_{infl} . As long as the second term in the braces in (4.3) is large, that is, as long as the initial deflection is small and/or the angle of sweep-back is large, the parabola Q is soaring over the U axis and the $q^* = q^*(U)$ curves increase monotonically with U . For $A_0^* = [8g(\varphi)/\mu^2 \Omega]^{1/2}$ there is $U_1^{xt} = U_2^{xt}$, and this double root corresponds to a stationary value of $q^*(U)$ at which the curve $q^* = q^*(U)$ has an inflection point with a horizontal tangent. The latter curve represents a greater lower bound for the curves $q^* = q^*(U)$, which display a loop associated with a multiple-valuedness of the inverse function $U = U(q^*)$. From then on, the parabolas Q intersect the U axis. This is clearly visible, e.g., in Fig. 3 in which $A_0^* = 3$ corresponds to a value of A_0^* less than the critical value (associated with a horizontal tangent at the inflection point) while $A_0^* = 5$ is greater than the critical value of A_0^* . Figures 2, 3, and 4 display the dependence of the reduced load

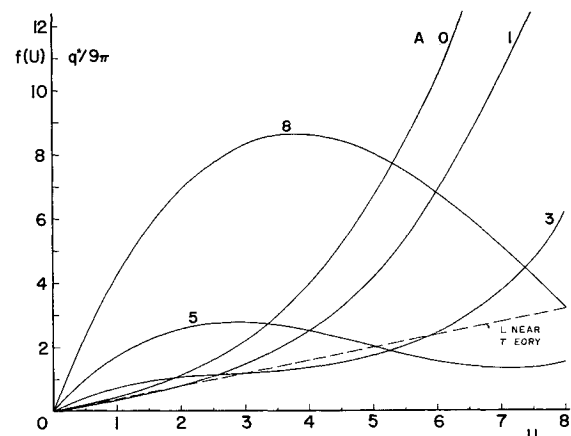


Fig. 3 Load or control function vs deflection U for a rhombic panel ($\varphi = 45^\circ$) and various values of initial deflection A_0^*

[†] It should be noted that some misprints in this equation as well as in Sec. 21 of Ref. 11 need correction.

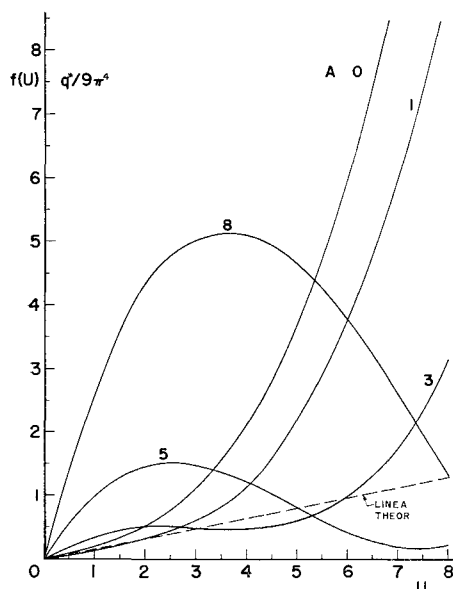


Fig. 4 Load or control function vs deflection U for a rhombic panel ($\varphi = 30^\circ$) and various values of initial deflection A_0^*

on the deflection parameter U for a rhombic panel and for various values of the dimensionless initial deflection A_0^* as well as of the angle of sweep-back φ^{**} . An inspection reveals the fact that, for a given initial deflection, the greater the value of φ , the greater the load which is required to produce a snap-through deflection. However, the snap-through occurs at a similar value of additional deflection. Moreover, the greater the angle φ , the greater the value of A_0^* at which higher states of equilibrium may occur.

5 Free Nonlinear Vibrations

We now proceed to discuss the general case of free nonlinear vibrations described by the equation

$$\ddot{U} + f(U) = 0 \quad (5.1)$$

with the restoring force (control term) $f(U)$ in the form of a cubic polynomial. Although an explicit integration of (5.1) through the use of elliptic integrals and functions is still possible, some important information of a qualitative character may be obtained using geometrical discussion in the phase plane $\ddagger\ddagger$.

We pose $V = \dot{U}$, and integrate (5.1). This yields the energy equation

$$(V^2/2) + F(U) = h \quad (5.2)$$

where

$$F(U) = (u_1/2)U^2 - (u_2/3)U^3 + (u_3/4)U^4 \quad (5.3)$$

is the potential energy of the system, and constant

$$h = (V_0^2/2) + F(U_0) \quad (5.4)$$

represents the total energy. Note that $F(U) = \int f(U)dU$ and that, at some initial time $\sigma = \sigma_0$, there is $U = U_0$ and $V = V_0$. It is also worth recalling that the graphs of the first derivative of the potential energy function are displayed in Figs 2-4.

^{**} Computations were provided by R. Beck, student at the University of Delaware.

^{\ddagger\ddagger} Compare, e.g., the books by Stoker (Ref. 14, Chap. 3) or McLachlan (Ref. 15, Chap. 9). An extensive analysis along these lines is given for nonlinear vibrations of rods and shallow axially symmetric shells in Ref. 16. The following discussion is modeled on all this work.

As is known, in order to analyze the integral curves (of constant energy) it is necessary to determine the singular points of the differential equation (5.1). The singularities correspond to rest positions of equilibrium since they are characterized by the conditions

$$V = 0 \quad f(U) = 0 \quad (5.5)$$

as displayed in a qualitative way in Fig. 5. In terms of the potential energy $F(U)$, they occur for values of U satisfying the condition $F'(U) = 0$, that is, at the points of extrema of potential energy (cf. Ref. 14, p. 49), and the sign of $f'(U)$ establishes the type of equilibrium. For future use, we note that, in view of (2.3), all the coefficients λ_i^* ($i = 1, 2, 3$) are also positive. Using this fact, we find that

$$f''(U) = (\mu^2\Omega/48)(U - A_0^*) \quad (5.6)$$

is negative in every sufficiently small vicinity of the origin, provided $A_0^* \neq 0$. Hence, the plate reveals a soft spring behavior near the origin for all values of the initial curvature except that equal to zero, when the spring behavior becomes hard. We write now (5.1) in the form

$$dV/dU = [-f(U)/V] \quad (5.7)$$

and compare (5.7) with the standard form

$$\frac{dV}{dU} = \frac{aU + bV + G_2(U, V)}{cU + dV + H_2(U, V)} \quad (5.8)$$

for application of the criteria of Poincaré (G_2 and H_2 vanishing like $U^2 + V^2$ as $U, V \rightarrow 0$). In the present case, we have

$$a = -u_1 \quad b = c = 0 \quad d = 1 \quad (5.9.1)$$

so that the discriminant

$$D \equiv (b - c)^2 + 4ad = -4u_1 < 0 \quad (5.9.2)$$

and

$$b + c = 0 \quad (5.9.3)$$

Bearing in mind that the singularities occur for values of $U = U_i^{\text{ing}}$ ($i = 1, 2, 3$), satisfying $F'(U) \equiv f(U) = 0$ (in other words, at points corresponding to points of intersection, or tangency, of the control characteristic and the U axis), we obtain easily

$$U_1^{\text{ing}} = 0 \quad (5.10)$$

$$U_{2,3}^{\text{ing}} = \frac{A_0^*}{2} \left\{ 3 \mp \left[1 - \frac{32g(\varphi)}{\mu^2\Omega(A_0^*)^2} \right]^{1/2} \right\}$$

where apparently

$$U_1^{\text{ing}} \leq U_2^{\text{ing}} \leq U_3^{\text{ing}} \quad (5.11)$$

An inspection of (5.10) reveals the fact that for large values of the second term in the brackets [Eq. (5.10)], that is, for small initial curvatures and/or for large values of the angle of sweep-back, there exists only one singular point located

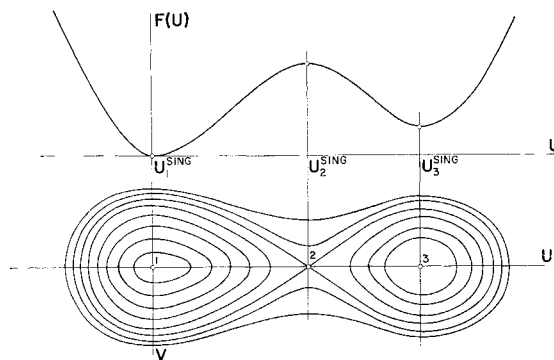


Fig. 5 Relation of singular points to potential energy

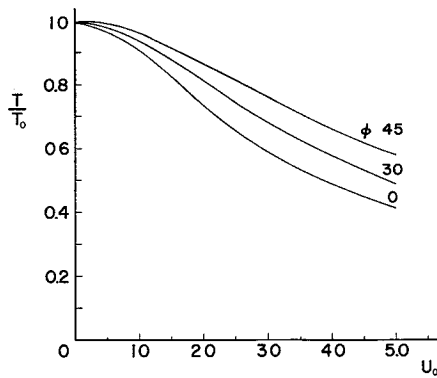


Fig 6 Relative period of nonlinear vibrations vs amplitude for a rhombic plate and various values of the angle φ

at the origin of coordinates For

$$A_0^* = 4/\mu(2g(\varphi)/\Omega)^{1/2} \quad (5.12)$$

there occurs a second singular point, besides $U = 0$, located at $U = \frac{3}{2}A_0^*$. Finally, if A_0^* is greater than the right-hand member of (5.12), we list three separate singular points

We now proceed to a classification of singularities of Eq (5.1)

A Singular Point $U = U_1^{\text{sing}}, V = 0$

Since, in this case, the discriminant is negative, the condition $b + c = 0$ no longer suffices to distinguish between a center and a spiral (see, e.g., Ref 14, p. 44). The derivative of the control term, however, df/dU , is positive at the origin so that the singular point is a center (compare point 1 in Fig 5; see also Ref 15, p. 205)

B Singular Point $U = U_2^{\text{ing}}, V = 0$

We observe that the change of origin from $U = 0$ to U_2^{sing} obtained by setting $U = U_2^{\text{ing}} + z$ replaces (5.7) by

$$\frac{dV}{dz} = -\frac{u_3 U_2^{\text{ing}}(U_2^{\text{ing}} - U_3^{\text{sing}})z + \dots}{V} \quad (5.13)$$

where the dots stand for higher-order terms in z which are disregarded. But, in the present case,

$$D = 4a = 4u_3 U_2^{\text{ing}}(U_3^{\text{ing}} - U_2^{\text{ing}}) > 0 \quad (5.14.1)$$

and

$$\Delta = ad - bc = a > 0 \quad (5.14.2)$$

Hence, the singularity is a saddle (compare point 2 in Fig 5). Since, specifically,

$$\Delta = U_2^{\text{ing}}(u_2^2 - 4u_1 u_3)^{1/2} \quad (5.14.3)$$

then, if $u_2 = 2(u_1 u_3)^{1/2}$, the saddle degenerates into a cusp

C Singular point $U = U_3^{\text{sing}}, V = 0$

The argument runs now closely parallel to that of the preceding case. A change of origin replaces (5.7) by

$$\frac{dV}{dz} = -\frac{u_3 U_3^{\text{sing}}(U_3^{\text{ing}} - U_2^{\text{ing}})z + \dots}{V} \quad (5.15)$$

with

$$D = 4a = 4u_3 U_3^{\text{sing}}(U_2^{\text{ing}} - U_3^{\text{ing}}) < 0 \quad (5.16.1)$$

and

$$b + c = 0 \quad (5.16.2)$$

The singular point may be thus either a center or a spiral

It may be easily verified, however, that

$$\left[\frac{df}{dz} \right]_{z=0} = U_3^{\text{ing}}(u_2^2 - 4u_1 u_3)^{1/2} > 0 \quad (5.17)$$

so that, in general, the singularity is a center (compare point 3 in Fig 5) and for $u_2 = 2(u_1 u_3)^{1/2}$ becomes a cusp. In the latter case, the second and third singularities coincide, and the potential energy curve suffers, at the corresponding point, an inflection with a tangent directed horizontally.

As is known, the period of oscillations T^* associated with either of the singularities of Eq (5.1) may be calculated by the line integral

$$T^* = \oint dU/V \quad (5.18)$$

to be taken along a closed energy curve in the direction of increasing time parameter t .

For a flat plate, say, rhombic for definiteness, the period of free nonlinear vibrations may be easily determined by an explicit integration. Recalling Eqs (3.3), and noting that in the present case $A_0^* = 0$ and $\mu = 1$, leads to

$$(d^2 U/d\sigma^2) + u_1 U + u_3 U^3 = 0 \quad (5.19)$$

where now

$$u_1 = \frac{2 + \sin^2 \varphi}{27(1 - \nu^2) \cos^4 \varphi} \quad u_3 = \frac{\lambda_1^* + \lambda_2^* + \frac{1}{8}}{144} \quad (5.20)$$

$$\lambda_1^* = \frac{1 + \sin^2 \varphi}{2(1 - \sin^2 \varphi)^2} \quad \lambda_2^* = \frac{25 + 16 \sin^2 \varphi}{(25 - 16 \sin^2 \varphi)^2}$$

By virtue of (5.2), the integral curves on the phase plane become

$$V^2 + u_1 U^2 + (u_3/2) U^4 = 2h \quad (5.21)$$

and they are symmetric with respect to both the coordinate axes. The only real singular point is that located at the origin and is a center.

Take as initial conditions, at $t = 0$, $A^* = U_0$ (so that $\tau(0) = 1$) and $V = \dot{U} = 0$. Hence U_0 represents the amplitude of oscillations. It is easily shown that, in the case considered, the period of the nonlinear oscillations becomes

$$T^* = 4/(u_1 + u_3 U_0^2)^{1/2} F[k, (\pi/2)] \quad (5.22)$$

where $F(k, \pi/2)$ is a complete elliptic integral of the first kind, with modulus $k^2 = \frac{1}{2}[1 + (u_1/u_3)U_0^{-2}]$ (compare Ref 15, p. 27). Since the period of free linear oscillations is

$$T_0 = 2\pi/(u_1)^{1/2} \quad (5.23)$$

the relative period of nonlinear oscillations appears finally as

$$\frac{T^*}{T_0} = \frac{2}{\pi[1 + (u_3/u_1)U_0^2]^{1/2}} F(k, \pi/2) \quad (5.24)$$

An inspection of (5.24) reveals the known fact that in virtue of the multiplier $[1 + (u_3/u_1)U_0^2]^{-1/2}$, the periodic time of nonlinear vibrations decreases with an increase of the amplitude U_0 . Figure 6 depicts the dependence of the relative period of free nonlinear vibrations on the amplitude of vibrations U_0 for various values of the angle of sweep-back φ . It is worth noticing that the corresponding curves become flatter for higher values of φ , so that a sweep-back of a plate makes the phenomenon of decreasing period less pronounced. However, even for the largest value of φ analyzed, that is, for $\varphi = 45^\circ$, the decrease of the period of vibrations is rather sharp, and for the amplitude, $U_0 = 3$ reaches nearly 25%. Clearly, a decrease of φ and an increase of U_0 influence the relative period T^*/T_0 in the opposite directions. Thus, by a suitable combination of the values of φ and U_0 , it is possible to set up the value of the period of vibrations on some desired

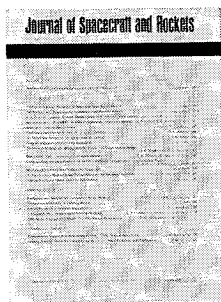
level Let us note again that the foregoing results concern a single mode, corresponding to what we consider to be approximately a fundamental mode [compare Eq (11)] Thus, until a more accurate than one term approximation is known, one has to bear in mind the limitations of the present solution

References

- ¹ Guest, J, "The buckling of uniformly compressed parallelogram plates having all edges clamped," Aeronautical Research Lab, Rept S M 172, Australia (1951)
- ² Wittrick, W H, "Buckling of oblique plates with clamped edges under uniform compression," Aeronaut Quart 4, Part 2, 151-163 (February 1953)
- ³ Wittrick, W H, "Buckling of oblique plates with clamped edges under uniform shear," Aeronaut Quart 5, Part 1 (May 1954)
- ⁴ Hasegawa, M, "On buckling of a clamped rhombic thin plate in shear," J Aeronaut Sci 21, 720 (1954)
- ⁵ Yoshimura, Y and Iwata, K, "Buckling of simply supported oblique plates," J Appl Mech 30, 363 (1963)
- ⁶ Dzygadlo, Z, "Stability of freely supported oblique plates under compression," Bul Mil Tekhn Akad 5, 81-92 (1956)
- ⁷ Grigoliuk, E I, "Vibration of a shallow circularly cylindrical panel exhibiting finite deflections," Prikl Mat Mekh 19, 376-382 (1955)
- ⁸ Chu, H-N and Herrmann, G, "Influence of large amplitudes on free flexural vibrations of rectangular elastic plates," J Appl Mech 23, 532-540 (1956)
- ⁹ Nash, W A and Modeer, J R, "Certain approximate analysis of the nonlinear behavior of plates and shallow shells," Intern Tech Rept 1, Dept of Engineering Mechanics, Univ of Florida (1959)
- ¹⁰ Hassert, J E and Nowinski, J, "Nonlinear transverse vibrations of a flat rectangular orthotropic plate supported by stiff ribs," Tech Rept 18, Univ of Delaware (1962); also *Proceedings of the Fifth International Symposium on Space Technology and Science* (to be published)
- ¹¹ Volmir, A S, "Flexible plates and shells," (Government Technical Publication—Theoretical Literature, Moscow, 1956), pp 58, 94, 112, and 208
- ¹² Timoshenko, S, *Theory of Plates and Shells* (McGraw-Hill Book Co, Inc, New York, 1940), p 321
- ¹³ Lekhnitski, S G, *Anisotropic Plates* (O G I Z, Moscow, 1957), p 375
- ¹⁴ Stoker, J J, *Nonlinear Vibrations* (Interscience Publishers, New York, 1957), Chap 3
- ¹⁵ McLachlan, N W, *Ordinary Non-Linear Differential Equations* (Clarendon Press, Oxford, England, 1958), Chap 9
- ¹⁶ Grigoliuk, E I, "Nonlinear vibrations and stability of shallow rods and shells," Izv Akad Nauk SSSR 3, 33 (1955)
- ¹⁷ von Kármán, T, "Festigkeitsprobleme in Maschinenbau," *Encyklopädie Math Wiss IV*, 348-351 (1910)

Journal of Spacecraft and Rockets

A publication of the American Institute of Aeronautics and Astronautics devoted to astronautical science and technology



Engineers and scientists in astronautics will find in the AIAA's new JOURNAL OF SPACECRAFT AND ROCKETS the blending of basic engineering system studies and technological

advances necessary for progress in space flight Featuring engineering studies substantiated by analysis and data this JOURNAL brings together—
Missions and systems analysis
Spacecraft missile launch vehicle and spaceplane design and development
Propulsion system development
Power elements and systems
Guidance and control
Materials and structural design
Life systems and human factors
Flight testing flight operations and GSE
Manufacturing and processing techniques

Performance testing and reliability
Engineering economic analyses
Edited by Dr Gordon L Dugger of Johns Hopkins Applied Physics Laboratory the journal publishes an average of 15 articles bimonthly together with many timely engineering notes Make the important work presented in the AIAA JOURNAL OF SPACECRAFT AND ROCKETS part of your professional thinking Subscriptions are \$3 00 a year to members and \$15 00 a year to non members Subscribe now

Mail to:
AIAA Subscription Department
1290 6th Ave New York N Y 10019

Please start my one year subscription to the JOURNAL OF SPACECRAFT AND ROCKETS

☐ Members \$3/yr
☐ Nonmembers \$15/yr

NAME _____

ADDRESS _____

CITY _____ STATE _____ ZIP CODE _____

All orders must be prepaid